It's about time: Circadian rhythm and metabolism

Schilperoort, M.

Circadian disruption by shifting the light-dark cycle negatively affects bone health in mice

Maaike Schilperoort, Nathalie Bravenboer, Joann Lim, Kathrin Mletzko, Björn Busse, Leo van Ruijven, Jan Kroon, Patrick C.N. Rensen, Sander Kooijman, Elizabeth M. Winter

The FASEB Journal (2019) 34: 1052-64

Abstract

The past decade, it has become evident that circadian rhythms within metabolically active tissues are very important for physical health. However, although shift work has also been associated with an increased risk of fractures, circadian rhythmicity has not yet been extensively studied in bone. Here, we investigated which genes are rhythmically expressed in bone, and whether circadian disruption by shifts in light-dark cycle affects bone turnover and structure in mice. Our results demonstrate diurnal expression patterns of clock genes (*Rev-erbα, Bmal1, Per1, Per2, Cry1, Clock*), as well as genes involved in osteoclastogenesis, osteoclast proliferation and function (*Rankl, Opg, Ctsk*) and osteocyte function (*c-Fos*) in bone. Weekly alternating light-dark cycles disrupted rhythmic clock gene expression in bone, and caused a reduction in plasma levels of procollagen type 1 amino-terminal propeptide (P1NP) and tartrate-resistant acidic phosphatase (TRAP), suggestive of a reduced bone turnover. These effects coincided with an altered trabecular bone structure and increased cortical mineralization after 15 weeks of light-dark cycles, which may negatively affect bone strength in the long term. Collectively, these results show that a physiological circadian rhythm is important to maintain bone health, which stresses the importance of further investigating the association between shift work and skeletal disorders.

Introduction

Our 24/7 society is dependent on shift work, which includes night shifts and rotating shift schedules. These working schedules result in a misalignment between the sleep-wake cycle and the internal biological clock, which is under control of the suprachiasmatic nucleus (SCN) in the hypothalamus, also referred to as the central 'master' clock. The SCN receives light signals from the eyes, and subsequently synchronizes circadian (i.e. 24 h) rhythms in all responsive tissues of the body. These tissue rhythms are driven by circadian clock genes, which promote rhythmic expression of many important tissue-specific genes and proteins [1, 2]. There is a substantial amount of evidence demonstrating the importance of circadian rhythm in biological functions of metabolic tissues such as liver, muscle and adipose tissue [3-5]. Accordingly, circadian disruption through shift work has been associated with numerous disorders related to a dysfunction in metabolic tissues, such as obesity, diabetes and cardiovascular disease [6-8]. In addition, shift work has been associated with a low bone mineral density and increased fracture risk [9, 10], which are both hallmarks of the bone disease osteoporosis. The personal burden of osteoporosis is high, with a significant decrease in quality of life and increased mortality in case of fractures [11, 12]. Nevertheless, the importance of circadian rhythm for skeletal health has not yet been extensively studied.

Healthy bone is constantly being remodeled, and this remodeling is important for bone growth and repair, as well as maintaining bone strength [13]. Bone is composed of a compact outer layer of cortical bone, and an inner structure of trabecular bone formed by a network of beams called trabeculae. Three main cell types reside in these bone structures and play an important role in bone remodeling: osteoclasts, osteoblasts and osteocytes. While osteoclasts degrade and resorb mineralized bone, osteoblasts produce bone matrix which is mineralized to form new bone [14]. Osteoblasts can communicate with osteoclasts by excreting receptor activator of nuclear factor κ-B ligand (RANKL), which binds to its receptor RANK on osteoclasts. Activation of RANK stimulates osteoclast differentiation, maturation and activity, thereby increasing bone resorption. Another protein secreted by osteoblasts is osteoprotegerin (OPG), which binds to RANKL and prevents it from interacting with RANK, thus preventing the bone from excessive resorption [15]. Osteocytes form an interconnected network within the bone tissue that senses mechanical stress. In response to these signals, osteocytes communicate with both osteoclasts and osteoblast to regulate their activity dependent on the mechanical needs of the bone tissue [16].

Physiological bone remodeling requires a balance between bone resorption by osteoclasts and bone formation by osteoblasts, which can be assessed through measuring bone turnover markers [17]. Recently, it has been shown that circulating bone turnover markers exhibit a circadian rhythm in humans [18], and are negatively affected by a combination of circadian disruption and sleep restriction [19]. Furthermore, genetic disruption of clock genes affects the bone phenotype in mice [20-24], suggesting a causal link between circadian physiology and bone health. However, whether mistimed light exposure in shift work is causally related to skeletal disorders remains to be elucidated. In this study, we aimed to investigate whether clock genes and genes involved in bone remodeling are rhythmically expressed in bones of mice, and examined whether circadian disruption through modeled shift work affects bone turnover and structure.

Materials and methods

Animals

Mouse studies were performed in APOE*3-Leiden.CETP mice, a well-established model for human-like lipoprotein metabolism [25], as they were also designed to examine effects of alternating light-dark cycles on lipid metabolism [26]. This way we could reduce the use of experimental animals. Eleven- to sixteen-week-old female APOE*3-Leiden.CETP mice fed a chow diet were killed at Zeitgeber time (ZT) 0, ZT6, ZT12 and ZT18 to assess circadian rhythmicity of bone. In addition, to evaluate effects of disturbance in circadian rhythmicity on bone, thirteen- to seventeen-week-old female APOE*3-Leiden.CETP mice fed a Western-type diet (35% energy from fat; supplemented with 0.1% cholesterol) were exposed to either regular light-dark cycles (LD), or weekly alternating light-dark cycles (LD-DL; i.e. complete reversal of the light and dark phase every week), as illustrated by Figure 1 (see 'Behavioral analysis' section for more information). Mice were exposed to 10 weeks of light intervention and killed three days after the last shift in light-dark cycle at ZT0 and ZT12 to evaluate effects of circadian disruption on gene expression in bone. These timepoints were chosen as most clock genes show a peak in amplitude either around ZT0 or ZT12 in peripheral tissues [27]. Tibiae were freshly isolated, flushed with PBS to remove the bone marrow and stored in RNAlater stabilization solution (ThermoFisher), followed by RNA isolation, cDNA synthesis and qRT-PCR analysis as described below. Mice were exposed for 15 weeks of light intervention and killed three days after the last shift in light-dark cycle from ZT0 to ZT6 to evaluate long-term effects of circadian disruption on bone turnover and structure. To this end, blood was collected to measure bone turnover markers, and femora were isolated, fixed in formalin and stored in 70% ethanol for histology, micro-CT (micro-computed tomography) analysis, mechanical testing and analysis of mineralization. Mouse experiments were performed in accordance with the Institute for Laboratory Animal Research Guide for the Care and Use of Laboratory Animals after having received approval from the University Ethical Review Board (Leiden University Medical Center, Leiden, The Netherlands).

Behavioral analysis

Throughout the entire study, behavioral activity patterns were assessed by housing mice in cages fitted with passive infrared detectors. Behavioral patterns per cage were analyzed by plotting actograms using ClockLab data analysis software (Actimetrics), as shown in Fig. 1. The recorded activity data was used to calculate total physical activity and physical activity per day in the light versus dark phase following a shift in light-dark cycle.

RNA isolation, cDNA synthesis and qRT-PCR

Tibiae were homogenised in TRIzol RNA isolation reagent (Roche Diagnostics), and total RNA was isolated according to the manufacturer's instructions. 1 μg of total RNA was reverse-transcribed using M-MLV reverse transcriptase (Promega), and qRT-PCR was performed with a SYBR Green Supermix on a CFX96 PCR machine (Bio-Rad). Primer sequences are available upon request. mRNA expression of genes of interest was normalized to mRNA expression of the housekeeping gene *Gapdh*.

P1NP, TRAP and corticosterone measurements

After sacrifice of the mice, blood was collected via cardiac puncture in EDTA-coated tubes. These samples were used to determine plasma concentrations of P1NP and TRAP using enzyme immunoassay kits (IDS) according to manufacturer's instructions. In week 3 of the study, blood

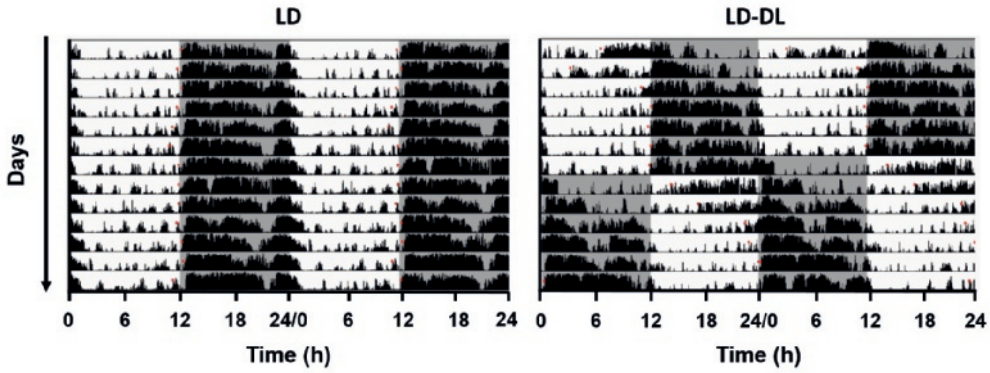

Figure 1. Schematic double-plotted actograms, illustrating the study setup. APOE*3-Leiden.CETP mice were exposed to either regular light-dark cycles (LD) or weekly alternating light-dark cycles (12 h shifts; LD-DL) to mimic shift work. Behavioral activity data was collected via passive infrared monitors, and used to generate actograms (i.e. a schematic representation of the activity over time). Representative double-plotted actograms are shown, in which a white background indicates the light phase (Zeitgeber time (ZT) 0-12), a grey background indicates the dark phase (ZT12-24), and black vertical bars indicate physical activity.

was collected via the tail vein in heparin-coated capillaries, on day 1, 3 and 5 after a shift in light-dark cycle at ZT0 and ZT12. Blood collection was performed in a stress-minimized manner (i.e. via a nick in the tail vein and within 2 min, to precede the stress-induced rise in corticosterone levels), as described before [28]. Corticosterone concentration was measured by ELISA according to the manufacturer's protocol (Corticosterone EIA, Immunodiagnostics).

TRAP histochemistry

Bones were fixed with formalin, decalcified for three weeks in 10% EDTA, paraffin embedded and cut into 5 µm sections. Sections were stained for TRAP using an acid phosphatase kit (Sigma-Aldrich), and counterstained with a Light Green solution. Osteoblasts were stained using a primary anti-osteocalcin antibody (ALX-210-333, 1:1000; Enzo Life Sciences) in combination with a goat anti rabbit secondary antibody (Dako). Sections were counterstained with haematoxylin. Slides were digitalized with Philips Digital Pathology Solutions (PHILIPS Electronics) for morphological measurement, and both osteoclast and osteoblast surface area was quantified using TrapHisto open source software [29].

Micro-CT analysis

Micro-CT analysis was performed to evaluate structural changes of the bone. Bones were scanned with a microcomputed tomography system (µCT 40; Scanco Medical AG) using 55 kV, 145 µA, 300 ms integration time and a resolution of 10 µm. Image processing included Gaussian filtering and segmentation with σ=0.8, support 1, threshold 430 mg hydroxyapatite (HA)/cm3 for trabecular parameters and 600 mg HA/cm3 for cortical parameters, respectively. For trabecular bone, a total of 150 slides (1.5 mm) starting from 0.1 mm distal to the growth plate were analyzed. For cortical bone, 25 slides above and 25 slides below the exact midpoint of the bone were analyzed (total 0.5 mm). Trabecular and cortical volumes of interest (VOI) were chosen by visual inspection. The morphometry of cortical and trabecular bone was performed with the program uct_evaluation v6.5-3 (Scanco Medical AG).

Mechanical testing by three-point bending

Three-point bending tests of femora were performed using a material testing device with a 0 N to 200 N force sensor (Z.2.5/TN1S, Zwick/Roell). After rehydration in saline for two days, the femora were placed with the anterior surface facing up on two fulcra separated by 7 mm. They were loaded perpendicularly to the midshaft of the bone with a rounded-off indenter that was lowered with a displacement rate of 0.01 mm/s. The response to this load was recorded in force-displacement curves. Maximum load (Fmax) and stiffness were calculated directly by the testing software (testXpert 10.1, Zwick GmbH & Co). Young's modulus was determined using the minimal moment of inertia of the midshaft from the Micro-CT analysis.

Analysis of mineralization

The bone mineral density distribution (BMDD) of femora was determined with a scanning electron microscope (ZEISS Crossbeam 340, ZEISS) using quantitative backscattered electron imaging (qBEI) as described before [30]. The femurs were dehydrated in ascending alcohol concentrations and embedded into polymethyl methacrylate (PMMA). The PMMA blocks were grounded coplanarly, polished and carbon coated. The microscope was run at 20 kV with a constant working distance of 20 mm. qBEI images of both the cortical and trabecular bone were made with a magnification of 600x and a pixel resolution of 0.4 µm. The gray level was calibrated using carbon and aluminium. The bone mineralization distribution was characterized by the mean and peak of the gray value distribution, which correspond to the mean calcium content (CaMean (wt%)) and peak calcium content (CaPeak (wt%)). The region of interest (ROI) was set over 0.38 mm along the shaft starting from 0.35 mm distal to the growth plate. Cortical and trabecular bone were separated visually.

Statistical analysis

All data are expressed as means ± SEM. Statistical analysis was performed using GraphPad Prism (version 7.02 for Windows). Means were compared using the Student's T-test, correcting for multiple comparisons using the Holm-Sidak method when applicable. Pearson correlation analysis was performed to examine potential linear relationships between variables. Differences between groups were considered statistically significant at $P < 0.05$. Rhythm analyses were performed by fitting a sine wave (Y = BaseLine + Amplitude * sin (Frequency * X + PhaseShift)) to the data. Gene expression was considered rhythmic if the 95% confidence interval of the amplitude did not include 0.

Results

Bone exhibits a potent circadian rhythm in gene expression

In tibiae bone samples, expression patterns of clock genes *Rev-erbα* (or *Nrd1*, nuclear receptor subfamily 1 group D member 1), *Bmal1* (brain and muscle Arnt-like protein-1), *Clock* (circadian locomotor output cycles kaput), *Per1* (period circadian regulator 1), *Per2* (period circadian regulator 2) and *Cry1* (cryptochrome circadian regulator 1) showed a circadian rhythm (Fig. 2A), with the rhythm in *Rev-erbα* and *Bmal1* being the most pronounced (more than a 3-fold difference in gene expression between the highest and lowest point). To evaluate a functional rhythm of bone cells, we measured diurnal expression of various bone-related genes. Expression of *Rankl, Opg, c-Fos* and *Ctsk* (cathepsin K) all followed a circadian pattern (Fig. 2B). At the start of the light phase, markers for osteoclast function *Ctsk* and *Rankl* showed the highest expression. Expression of *Opg* was lowest at the start of the light phase. *c-Fos*, which is

expressed by osteocytes, is the highest in the middle of the dark period. Expression of *Runx2* (runt-related transcription factor 2), *Nfatc* (nuclear factor of activated T-cells), *Rank* and *Col1a1* (collagen type I α) was not rhythmic (Fig. 2B; data not shown).

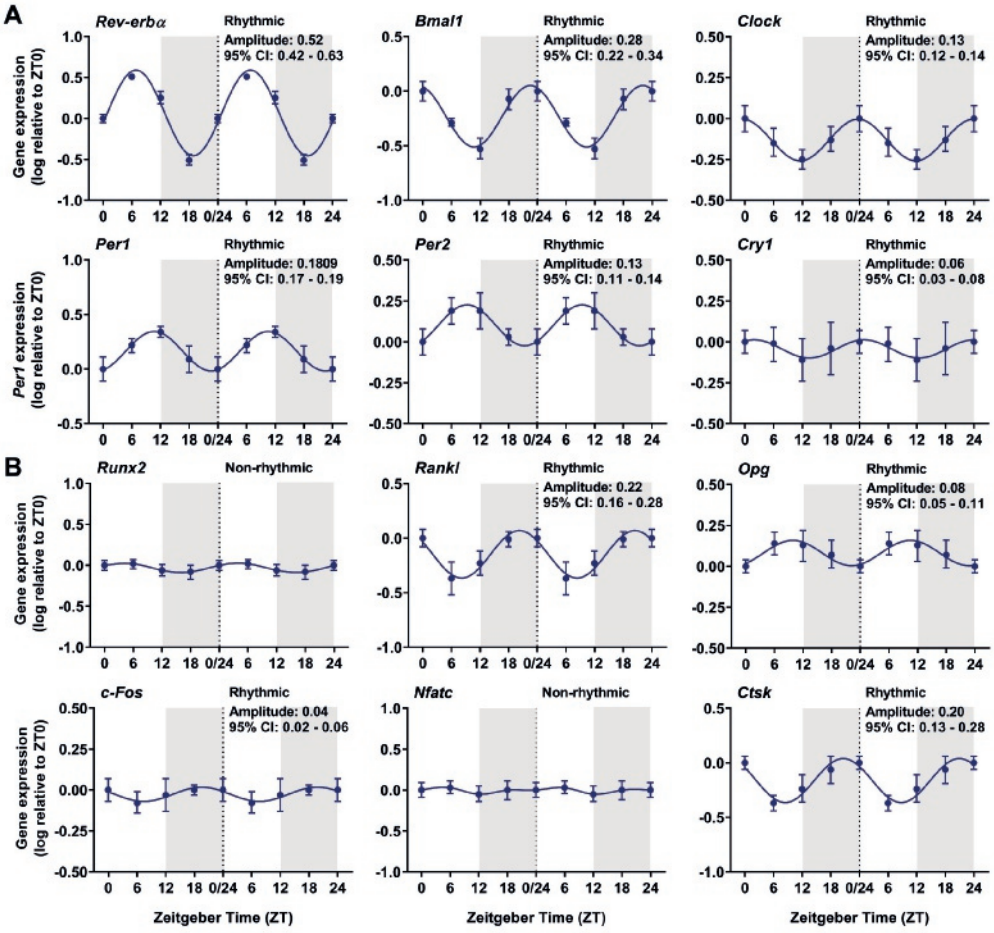

Figure 2. Bone shows rhythmic expression of clock and bone-related genes. (A, B) Mice were killed at Zeitgeber time (ZT) 0, ZT6, ZT12 and ZT18 (denotation of time in which ZT0 = lights on, and ZT12 = lights off) to assess circadian rhythmicity of clock genes (A) and bone-related genes (B) in tibiae (n = 7). Data points were log-transformed and double plotted from the dotted lines. Light and grey areas represent the light and dark phase, respectively. Rhythm analyses were performed by fitting a sine wave to the data and evaluating the confidence interval (CI) of the amplitude. Data represent means ± SEM.

Weekly alternating light-dark cycles disrupt circadian rhythm in bone

Next, we exposed mice to either regular light-dark cycles (LD), or weekly alternating light-dark cycles (LD-DL) for a period of 10 weeks, to evaluate effects of circadian disturbance on gene expression in bone. We killed the mice three days after the last shift in light-dark cycle, when they are not yet fully acclimated to their new rhythm (as shown in Fig. 1 with respect to activity rhythms). At this time point, expression of clock genes was disrupted in LD-DL mice (Fig.

3A), with significant differences in rhythm amplitude (ZT0-ZT12; the beginning of the light phase versus the beginning of the dark phase) of *Rev-erbα, Bmal1, Clock* and *Cry1* between LD-DL mice and LD controls (see Suppl. Table 1 for the rhythm amplitude and corresponding P-values). It also appeared that rhythm in bone-related genes such as *Opg, c-Fos* and *Ctsk* was attenuated by alternating light-dark cycles (Fig. 3B), but differences in rhythm amplitude of these genes were not significant (Suppl. Table 1).

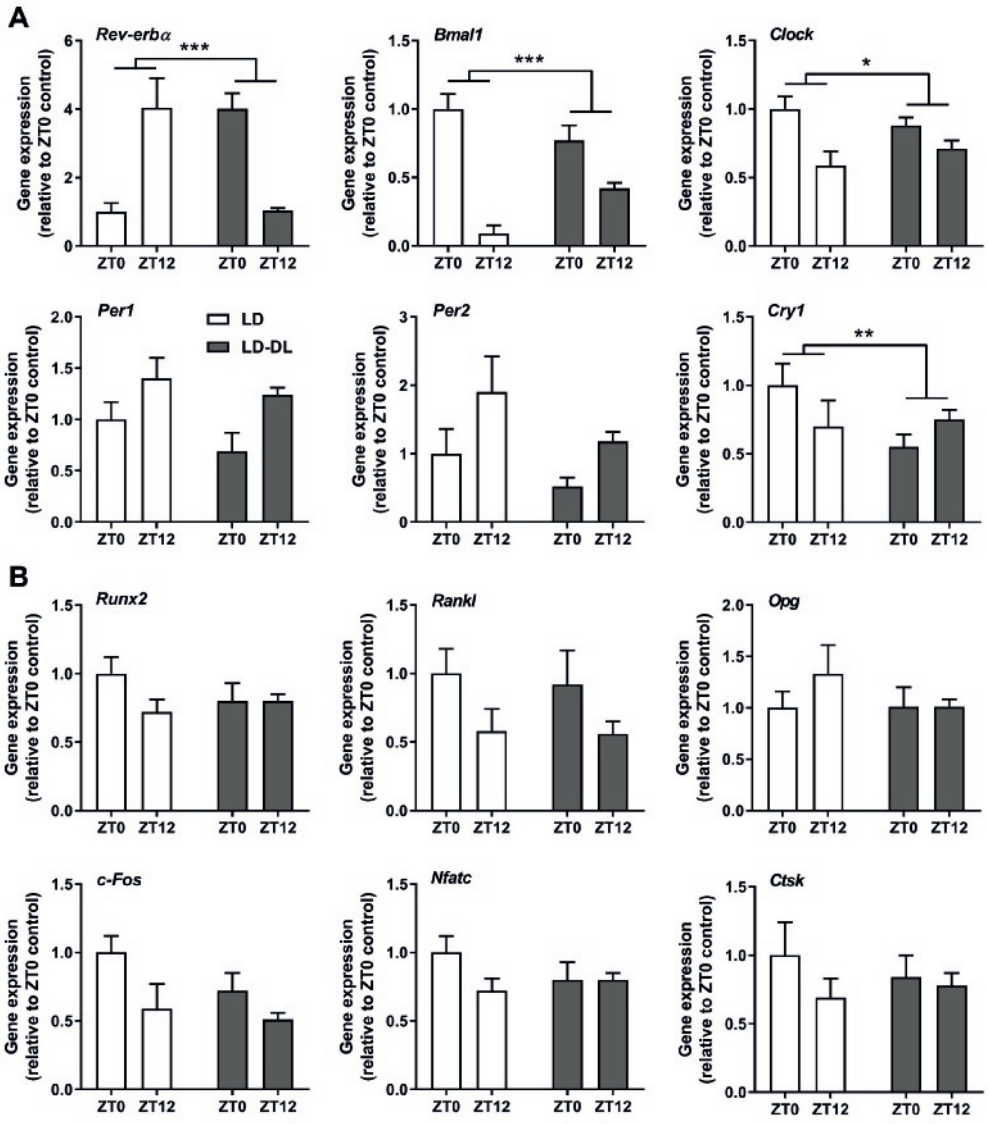

To evaluate whether circadian disruption would affect bone health on a longer-term, we exposed mice to weekly alternating light-dark cycles for a total period of 15 weeks. Alternating light-dark cycles did not affect total food intake (Fig. 4A), physical activity (Fig. 4B) or body weight (Fig. 4C) throughout the entire study period. Also, weight of metabolic organs (i.e. the liver, gonadal white adipose tissue (gWAT) and interscapular brown adipose tissue (iBAT)) was similar between LD-DL mice and LD controls at endpoint (Fig. 4D).
Next, we examined the effect of alternating light-dark cycles on two important mediators of peripheral circadian rhythm: the sympathetic nervous system and glucocorticoid hormone. Histological analysis of bone marrow revealed no effect of alternating light-dark cycles on tyrosine hydroxylase expression, a marker for sympathetic innervation (Fig. 4E). Plasma levels of corticosterone, the primary glucocorticoid in mice, were strongly rhythmic in LD control mice, with a 10-fold difference between morning (ZT0) and evening (ZT12) levels (Fig. 4F). In LD-DL mice, corticosterone rhythm was markedly disrupted on day 1 after a shift in light-dark cycle, but restored after 3 days. This was validated by two-way ANOVA analysis, which revealed a significant Time, Group and Interaction effect on day 1, while the factors Group and Interaction lost their significance on day 3 (Suppl. Table 2). Along with the disruption in corticosterone rhythm, we observed disruptions in behavioral activity of LD-DL mice. While LD mice were predominately active during the dark period, LD-DL mice were mostly active during the light period on day 1 after a shift in light-dark cycle. On day 3, rhythm in physical activity was somewhat restored, although still not to the extent of LD mice (Suppl. Table 2). Together, these data indicate that weekly shifts in light-dark cycle affect the circadian timing system and disrupt rhythmic gene expression in bone.

Circadian disruption affects bone turnover and structure

To evaluate whether the observed gene expression changes not only reflect a shift in acrophase (i.e. the timing of circadian amplitude), but could affect bone turnover and structure on the long-term, we measured bone turnover markers P1NP and TRAP in mice exposed to 15 weeks of light intervention. Plasma levels of P1NP were reduced in LD-DL mice versus LD controls (Fig. 5A), indicative of reduced bone matrix production by osteoblasts. However, staining of the osteoblast marker osteocalcin in femora revealed an increase in osteoblasts on the trabecular bone surface of LD-DL mice (Fig. 5B and C). This suggests that the decrease in P1NP is the result of an altered osteoblast function or activity rather than a decrease in the amount of osteoblasts. Plasma levels of TRAP, a marker of active osteoclasts, were also reduced in LD-DL mice compared to LD controls (Fig. 5D). This is supported by TRAP histochemistry (Fig. 5E and F), which showed a non-significant decrease in the amount of osteoclasts on the trabecular bone surface of LD-DL mice. These results indicate a reduction in both bone formation and resorption in mice exposed to alternating light-dark cycles.

≪ **Figure 3. Alternating light-dark cycles disrupt rhythmic clock gene expression in bone.** (A, B) Mice exposed to either a regular light-dark cycle (LD) or weekly alternating light-dark cycles (LD-DL) were killed after 10 weeks at Zeitgeber time (ZT) 0 (lights on) and ZT12 (lights off), three days after the last shift in light-dark cycle, to assess expression of clock genes (A) and bone-related genes (B) in tibiae. Differences in rhythm amplitude (ZT0-ZT12) were compared between LD-DL mice and LD controls (n = 8-9 per time point per group). Data represent means ± SEM. *P $<$ 0.05, **P $<$ 0.01, ***P $<$ 0.001 compared to the control group, according to the Student's T-test.

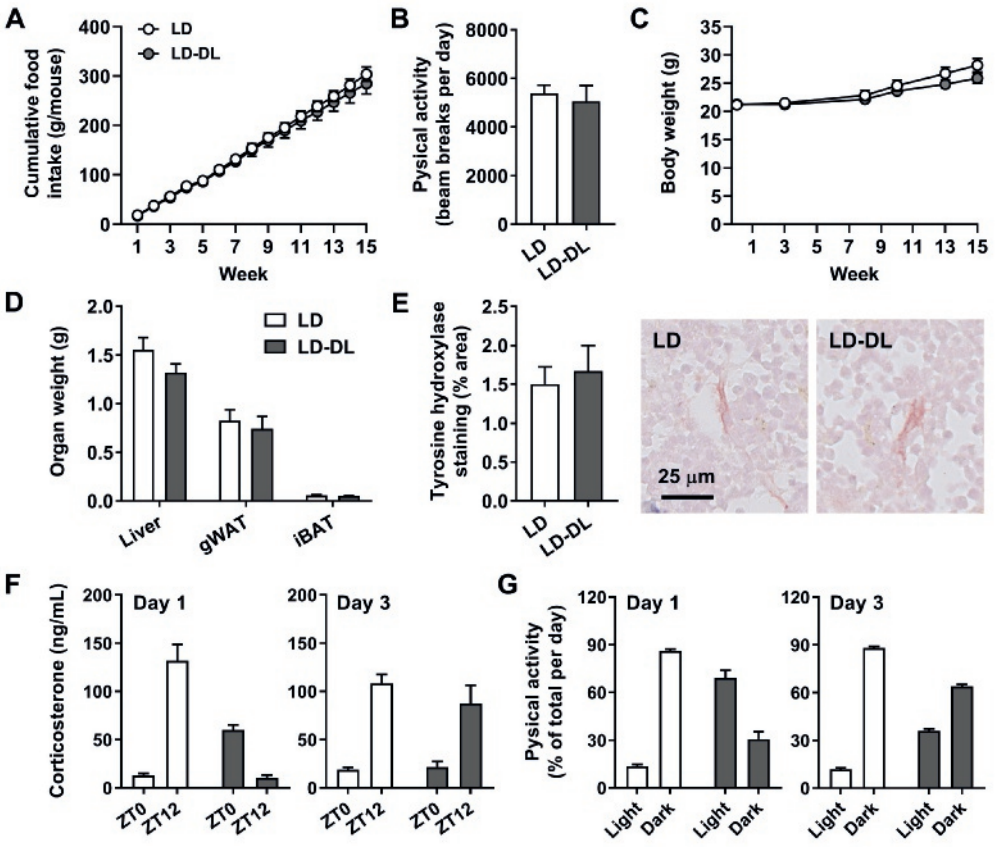

Figure 4. Alternating light-dark cycles disrupt rhythm in physical activity and corticosterone, without affecting metabolic parameters. Mice were exposed to 15 weeks of normal light-dark cycles (LD) or weekly alternating light-dark cycles (LD-DL), and killed three days after the last shift in light-dark cycle from ZT0 to ZT6 (n = 8 mice per group, n = 2 cages per group). (A) Cumulative food intake was measured per cage and expressed as gram per mouse. (B) Physical activity of each cage was measured via passive infrared monitors and the average activity over the whole study period was calculated. (C) Body weight was measured throughout the study (n = 8 mice per group). (D) Weight of the liver, gonadal white adipose tissue (gWAT) and interscapular brown adipose tissue (iBAT) was determined at endpoint (n = 8 per group). (E) Decalcified femora were stained for tyrosine hydroxylase (TH) as a marker for sympathetic innervation, and counterstained with haematoxylin. Digital images were used to quantify the relative TH-positive area in bone marrow (n = 6 mice per group). (F) Physical activity data was used to calculate the amount of activity in the light versus dark phase per cage, in week 3 on day 1 and 3 after a shift in light-dark cycle. (G) In week 3 of the study, plasma was collected from mice at lights on (ZT0) and lights off (ZT12) on day 1 and 3 after a shift in light-dark cycle to measure circulating corticosterone levels (n = 8 mice per group). Data represent means ± SEM. Data from Fig. 4F and G was compared by two-way ANOVA, of which P-values are reported in Suppl. Table 2.

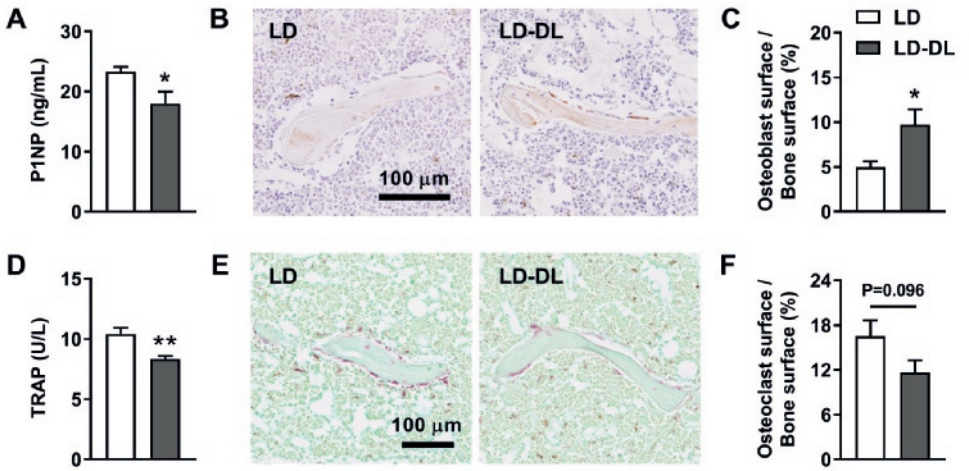

Figure 5. Alternating light-dark cycles affect bone turnover markers. (A) Plasma levels of pro-collagen type 1 amino-terminal propeptide (P1NP) were evaluated at end point, after 15 weeks of normal light-dark cycles (LD) or weekly alternating light-dark cycles (LD-DL) (n = 8 per group). (B, C) Decalcified femora were stained for osteocalcin to visualize osteoblasts, and counterstained with haematoxylin. Digital images were used to quantify the relative osteoblast surface area (n = 6 per group). (D) Plasma levels of tartrate-resistant acidic phosphatase (TRAP) were measured at end point (n = 8 per group). (E, F) Decalcified femora were stained for TRAP to visualize osteoclasts, and counterstained with Light Green. Stained slides were digitalized and used to quantify the relative osteoclast surface area (n = 6 per group). For all measurements, mice were killed three days after the last shift in light-dark cycle, from ZT0 to ZT6. Data represent means ± SEM. *P $<$ 0.05, **P $<$ 0.01 compared to the LD control group, according to the Student's T-test.

Next, we aimed to evaluate long-term effects of circadian disturbance on bone structure, strength and mineralization. Bone weight (Fig. 6A) and length (Fig. 6B) were non-significantly reduced in LD-DL mice. Micro-CT analysis was performed to measure parameters of both cortical and trabecular bone structure, listed in Table 1. Alternating light-dark cycles did not affect cortical parameters, such as cortical bone volume (Ct.BV; Fig. 6C) and cortical thickness (Ct.Th; Fig. 6D). Strength of the cortical bone as determined by mechanical testing was also not affected by the light intervention (Table 2). On the other hand, trabecular bone volume (BV/TV) tended to be increased in LD-DL mice versus LD controls (Fig. 6E). Accordingly, trabecular number (Tb.N) was increased (Fig. 6F) and trabecular spacing (Tb.Sp) was decreased (Table 1). These structural changes can also be appreciated from representative micro-CT images of trabecular bone shown in Fig. 6G. We measured the bone mineralization density distribution (BMDD) of both the cortical and trabecular bone by quantitative backscattered electron imaging (qBEI). The cortical BMDD showed a shift to the right in LD-DL mice compared to LD controls (Fig. 6H), with an increased mean calcium content (CaMean; Fig. 6I) and peak calcium content (CaPeak; Fig. 6J, also illustrated by dashed lines in the BMDD of Fig. 6H), demonstrating increased bone mineralization. The same tendencies were observed in trabecular bone (Fig. 6K-M).

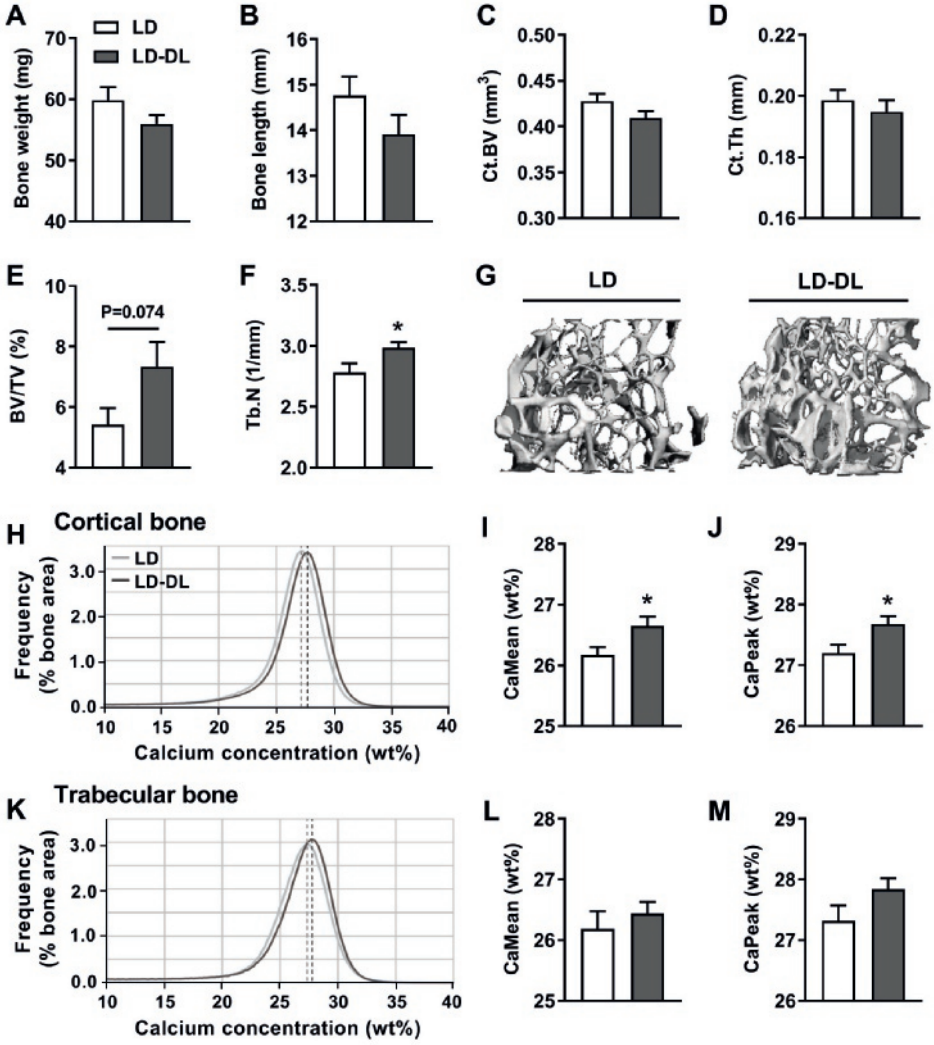

Figure 6. Alternating light-dark cycles modulate trabecular bone structure and increase bone mineralization. (A, B) Weight and length of whole femora bones was measured at end point, after 15 weeks of normal light-dark cycles (LD) or weekly alternating light-dark cycles (LD-DL) (n = 6-8 per group). (C-F) Micro-CT analysis was used to assess cortical bone volume (Ct.BV), cortical thickness (Ct.Th), trabecular bone volume (BV/TV) and trabecular number (Tb.N) (n = 7-8 per group). (G) Representative micro-CT images of the trabecular bone structure are shown. (H-M) qBEI was used to determine the bone mineralization density distribution (BMDD) of cortical (H) and trabecular (K) bone, characterized by the mean calcium content (CaMean) (I, L) and peak calcium content (CaPeak, as illustrated by dashed lines in the BMDD graph) (J, M) (n = 8 per group). Data represent means ± SEM. *$P < 0.05$ compared to the LD control group, according to the Student's T-test.

Table 1. Micro-CT analysis of bones from LD and LD-DL mice.

Parameter	LD (mean ± SEM)	LD-DL (mean ± SEM)
Cortical structure		
Ct.BV (mm^3)	0.43 ± 0.01	0.41 ± 0.01
Ct.BS (mm^2)	4.12 ± 0.08	4.10 ± 0.05
BS/BV (mm^2/mm^3)	9.85 ± 0.16	10.03 ± 0.18
Ct.Th (mm)	0.199 ± 0.003	0.195 ± 0.004
BMD (cortical)	1178.6 ± 10.9	1158.1 ± 7.8
Trabecular structure		
BV/TV (%)	5.42 ± 0.55	7.33 ± 0.83
Conn.Den. ($1/mm^3$)	30.4 ± 4.3	44.1 ± 5.2
SMI	2.99 ± 0.06	2.71 ± 0.16
Tb.N (1/mm)	2.78 ± 0.07	2.99 ± 0.04*
Tb.Th (mm)	0.0482 ± 0.003	0.0486 ± 0.001
Tb.Sp (mm)	0.36 ± 0.01	0.33 ± 0.01*
BMD (trabecular)	894.4 ± 10.0	906.4 ± 4.1

BMD, bone mineral density; BS/BV, cortical area fraction; BV/TV, trabecular bone volume; Conn.Den., connectivity density; Ct.BS, cortical bone surface; Ct.BV, cortical bone volume; Ct.Th, cortical thickness; SMI, structure model index; Tb.N, trabecular number; Tb.Sp, trabecular spacing; Tb.Th, trabecular thickness. *$P < 0.05$ compared to the control group, according to the Student's T-test.

Table 2. Mechanical testing of bones from LD and LD-DL mice.

Parameter	LD (mean ± SEM)	LD-DL (mean ± SEM)
Mechanical testing		
Fmax (N)	14.37 ± 0.44	14.35 ± 0.23
Stiffness (N/mm)	112.0 ± 2.7	108.4 ± 2.3
Young's modulus (kN/mm^2)	5.60 ± 0.20	6.00 ± 0.09

Fmax, the highest load that the bone can withstand; Stiffness, measure of resistance to the applied displacement; Young's modulus, resistance to elastic deformation.

Discussion

In this study, we investigated the importance of circadian rhythms for bone health. We demonstrated that bone shows clear diurnal expression patterns of clock genes and bone-related genes. Furthermore, our results indicate that disturbing circadian rhythm by shifts in light-dark cycles affects the number and function of osteoclasts and osteoblasts, resulting in a decreased bone turnover and alterations in bone structure and mineralization that may negatively affect bone strength in the long-term.

We demonstrated rhythmic oscillations in clock gene expression in bone that are very similar to those observed in other tissues, such as adipose tissue, liver and muscle [27]. In these tissues, rhythms in *Rev-erbα* and *Bmal1* also show the strongest amplitude compared to other clock genes, and all clock genes follow the same rhythmic pattern as now demonstrated in bone. The importance of rhythm in clock gene expression for bone has been established previously by the presence of a bone phenotype in clock gene knockout mice. Mice lacking *Clock* or *Bmal1* have a reduced bone mass [21, 24], while *Per1/2* and *Cry1/2* double knockout mice have an increased bone mass [20], indicating involvement of clock genes in bone turnover. This is supported by our data demonstrating a rhythm in the expression of various bone-related genes. Of these genes, *Ctsk, Rankl* and *Opg* showed the strongest rhythm. Osteoclasts express *Ctsk*, which encodes the protease cathepsin K involved in bone resorption. *Ctsk* showed the highest expression at the onset of the light phase, suggesting increased bone resorption at this time. In line with this, expression of the osteoclast activator *Rankl* was high, while expression of the RANKL inhibitor *Opg* was low at light onset. The fact that genes involved in osteoclast function were found to be most rhythmic suggests osteoclasts may be particularly important in mediating circadian rhythm of bone tissue. Nonetheless, we also found oscillations in genes expressed by osteocytes and osteoblasts, suggesting presence of rhythm in all major bone cell types, which collectively may contribute to rhythmic bone remodeling [31].

It is currently unknown which internal cues can regulate rhythm in bone tissue. In response to light, the SCN is able to synchronize rhythm in peripheral tissues through regulation of behavioral rhythms (e.g. physical activity and fasting/feeding behavior), the autonomous nervous system and hormonal cues. Physical activity can directly affect bone remodeling through mechanical loading that is sensed by a network of osteocytes in the bone [32], and results in upregulation of the gene *c-Fos* [33]. We found a rhythmic *c-Fos* expression in bone, with the highest expression in the middle of the dark period, which is the active phase of mice. These results are consistent with *c-Fos* being induced in osteocytes by mechanical loading, and support a role of physical activity in rhythmic bone remodeling. Shifting light-dark cycles disrupted behavioral rhythm in mice, which could have affected the circadian clock in bone. Moreover, *in vitro* studies have demonstrated an important role for sympathetic innervation and glucocorticoid hormone for bone rhythm. Treatment of osteoblasts with the β-adrenergic receptor agonist isoprenaline promotes rhythmic oscillations in clock genes [34, 35], and the synthetic glucocorticoid dexamethasone has been shown to induce a rhythm in cultured osteoclasts and osteoblasts [35, 36]. In our study, we did not observe an effect of circadian disruption through light-dark shifts on the expression of tyrosine hydroxylase, a marker of sympathetic innervation, in bone. We did, however, observe a profound disturbance in the rhythm of the glucocorticoid hormone corticosterone following shifting light-dark cycles. Considering the important role that glucocorticoids play in regulating cell intrinsic rhythm, disturbance of glucocorticoid rhythm could (in part) underlie the observed disruption of the molecular clock in bone. However, future studies are needed to investigate whether

glucocorticoid rhythm is indispensable for rhythmic bone metabolism.

To further elucidate the importance of a physiological circadian rhythm for bone health, we measured bone turnover markers in mice subjected to circadian disruption by shifts in the light-dark cycle. Circadian disruption reduced bone turnover, evident by reduced plasma levels of the bone formation marker P1NP and the bone resorption marker TRAP. This is in line with the only intervention study performed in humans so far, that showed a reduction in P1NP as a result of a combination of sleep restriction and circadian disruption [19]. Furthermore, shifting light-dark cycles affected the trabecular bone structure, demonstrated by an increase in trabecular number and a decrease in trabecular spacing, accompanied by a trend towards an increased trabecular bone volume. This finding was surprising, as osteoporosis is characterized by a decrease in trabecular bone volume. This discrepancy might be explained by the fact that bones of mice show skeletal growth between 2 and 12 months of age (from early adult to middle age), which is accompanied by a natural decrease in relative trabecular bone volume and number and an increase in trabecular spacing [37, 38]. We exposed mice to light-dark shifts from 4-8 months of age and observed an opposite effect on these parameters, suggesting that the bones of these mice show an impaired growth, consistent with the observed decrease in bone turnover markers. Thus, circadian disruption may differentially affect trabecular bone structure in an age-dependent manner. Further research is required to investigate the impact of shifting light-dark cycles on bone quality in middle-aged mice in which bone remodeling is independent of skeletal growth.

While trabecular bone does contribute to bone strength [39], cortical bone bears the main part of the mechanical load [40]. Cortical bone structure was not significantly affected in our study, in which mice were exposed to 15 weeks of light intervention. Of note, the rate of bone remodeling is proportional to the surface area [41], which is greater for trabecular bone as compared to cortical bone. This makes cortical bone less responsive to changes in bone turnover [42]. Thus, a longer study duration perhaps could reveal additional effects of circadian disruption on cortical bone structure. Although cortical bone structure was not yet affected in our study, we did observe changes in cortical bone mineralization in mice exposed to shifting light-dark cycles. An optimal bone mineralization is required for bone stiffness, strength and toughness [43], and deviations in mineralization have been observed in a variety of bone diseases [44]. Although its exact role in bone physiology is still debated [45], osteocalcin has been reported to promote mineralization [46]. As we observed an increased osteocalcin staining in mice exposed to shifts in light-dark cycles, this could indicate changes in the mineralization process. Indeed, circadian disruption increased mineralization of cortical bone, which corresponds to an increased bone stiffness and brittleness. An increased mineralization has also been observed in bone of patients with osteoporosis, resulting in accumulation of microdamage and increased fracture risk [47, 48]. Although mechanical properties were still adequate to maintain cortical bone strength in our study, in the long-term the observed changes in mineralization could contribute to a decreased bone strength and increased fracture risk [48].

We performed our experiments in APOE*3-Leiden.CETP mice on a Western-type diet, as we also aimed to investigate effects of circadian disruption on lipid metabolism [26]. The increased levels of plasma lipids and cholesterol in these mice could have interacted with circadian disruption to deteriorate bone health, since lipid-rich diets have been shown to affect both bone metabolism and circadian rhythm [49, 50]. It would be of interest to study whether shifting light-dark cycles similarly affects bone health in metabolically healthy wildtype mice, or whether an additional metabolic challenge is required to observe effects of circadian disruption on bone. Furthermore, we specifically used female mice for our study. Although osteoporosis primarily

occurs in women [51], it is currently unknown whether effects of circadian disruption on bone health differ between men and women, which requires further investigation.
Taken together, we demonstrate that a relatively mild intervention of mistimed light exposure alters trabecular and cortical bone, which could explain the association between circadian disruption by means of shift work and osteoporosis in humans. Osteoporosis affects more than 200 million people worldwide, and osteoporotic fractures often result in chronic pain, long-term disability and even early death [52]. For a long time, osteoporosis has been thought of as part of the normal ageing process. However, the past decades both nonmodifiable (e.g. gender, ethnicity) and modifiable (e.g. nutrition, body weight, sun exposure) risk factors for osteoporosis have been well-defined [53]. Our work demonstrates that chronic rhythm disruption as occurs in shift work is an important additional risk factor. Of note, approximately 20% and 30% of workers in Europe and the U.S. participate in shift work, respectively [54, 55]. This high prevalence emphasizes the necessity of further research on the risk of skeletal disorders associated with circadian disturbances, as well as underlying mechanisms. This could be of great importance to develop novel behavioral and/or pharmacological strategies to prevent bone disease in shift workers.

Acknowledgements

This work was supported by a personal grant of the Leiden University Fund / Elise Mathilde Fund to EMW and by a personal grants from the Board of Directors of Leiden University Medical Center to MS. Additionally, this work was supported by the Dutch Heart Foundation (grant 2017T016 to SK) and the European Foundation for the Study of Diabetes (grant RS FS 2016_3 to SK). We thank Lianne van der Wee-Pals, Hetty Sips, Trea Streefland, Cheraine Bouten, Isabel Mol and Chris van der Bent (Division of Endocrinology, Department of Medicine, LUMC, Leiden, The Netherlands), and Huib van Essen (Department of Clinical Chemistry, Amsterdam University Medical Center, Amsterdam, The Netherlands) for their excellent technical assistance.

References

1. Miller, B.H., E.L. McDearmon, S. Panda, K.R. Hayes, et al. Circadian and CLOCK-controlled regulation of the mouse transcriptome and cell proliferation. Proc Natl Acad Sci U S A. 2007;104(9):3342-7.
2. Panda, S., M.P. Antoch, B.H. Miller, A.I. Su, et al. Coordinated transcription of key pathways in the mouse by the circadian clock. Cell. 2002;109(3):307-20.
3. Mukherji, A., S.M. Bailey, B. Staels, and T.F. Baumert. The circadian clock and liver function in health and disease. J Hepatol. 2019;71(1):200-211.
4. Harfmann, B.D., E.A. Schroder, and K.A. Esser. Circadian rhythms, the molecular clock, and skeletal muscle. J Biol Rhythms. 2015;30(2):84-94.
5. Kiehn, J.T., A.H. Tsang, I. Heyde, B. Leinweber, et al. Circadian Rhythms in Adipose Tissue Physiology. Compr Physiol. 2017;7(2):383-427.
6. Knutsson, A. and A. Kempe. Shift work and diabetes–a systematic review. Chronobiol Int. 2014;31(10):1146-51.
7. Sun, M., W. Feng, F. Wang, P. Li, et al. Meta-analysis on shift work and risks of specific obesity types. Obes Rev. 2018;19(1):28-40.
8. Torquati, L., G.I. Mielke, W.J. Brown, and T. Kolbe-Alexander. Shift work and the risk of cardiovascular disease. A systematic review and meta-analysis including dose-response relationship. Scand J Work Environ Health. 2018;44(3):229-238.
9. Feskanich, D., S.E. Hankinson, and E.S. Schernhammer. Nightshift work and fracture risk: the Nurses' Health Study. Osteoporos Int. 2009;20(4):537-42.
10. Quevedo, I. and A.M. Zuniga. Low bone mineral density in rotating-shift workers. J Clin Densitom. 2010;13(4):467-9.
11. Hernlund, E., A. Svedbom, M. Ivergard, J. Compston, et al. Osteoporosis in the European Union: medical management, epidemiology and economic burden. A report prepared in collaboration with the International Osteoporosis Foundation (IOF) and the European Federation of Pharmaceutical Industry Associations (EFPIA). Arch Osteoporos. 2013;8:136.
12. Lyles, K.W., C.S. Colon-Emeric, J.S. Magaziner, J.D. Adachi, et al. Zoledronic acid and clinical fractures and mortality after hip fracture. N Engl J Med. 2007;357(18):1799-809.
13. Hadjidakis, D.J. and Androulakis, II. Bone remodeling. Ann N Y Acad Sci. 2006;1092:385-96.
14. Mohamed, A.M. An overview of bone cells and their regulating factors of differentiation. Malays J Med Sci. 2008;15(1):4-12.
15. Boyce, B.F. and L. Xing. The RANKL/RANK/OPG pathway. Curr Osteoporos Rep. 2007;5(3):98-104.
16. Schaffler, M.B., W.Y. Cheung, R. Majeska, and O. Kennedy. Osteocytes: master orchestrators of bone. Calcif Tissue Int. 2014;94(1):5-24.
17. Greenblatt, M.B., J.N. Tsai, and M.N. Wein. Bone Turnover Markers in the Diagnosis and Monitoring of Metabolic Bone Disease. Clin Chem. 2017;63(2):464-474.
18. Redmond, J., A.J. Fulford, L. Jarjou, B. Zhou, et al. Diurnal Rhythms of Bone Turnover Markers in Three Ethnic Groups. J Clin Endocrinol Metab. 2016;101(8):3222-30.
19. Swanson, C.M., S.A. Shea, P. Wolfe, S.W. Cain, et al. Bone Turnover Markers After Sleep Restriction and Circadian Disruption: A Mechanism for Sleep-Related Bone Loss in Humans. J Clin Endocrinol Metab. 2017;102(10):3722-3730.
20. Fu, L., M.S. Patel, A. Bradley, E.F. Wagner, et al. The molecular clock mediates leptin-

regulated bone formation. Cell. 2005;122(5):803-15.
21. Samsa, W.E., A. Vasanji, R.J. Midura, and R.V. Kondratov. Deficiency of circadian clock protein BMAL1 in mice results in a low bone mass phenotype. Bone. 2016;84:194-203.
22. Takarada, T., C. Xu, H. Ochi, R. Nakazato, et al. Bone Resorption Is Regulated by Circadian Clock in Osteoblasts. J Bone Miner Res. 2017;32(4):872-881.
23. Xu, C., H. Ochi, T. Fukuda, S. Sato, et al. Circadian Clock Regulates Bone Resorption in Mice. J Bone Miner Res. 2016;31(7):1344-55.
24. Yuan, G., B. Hua, Y. Yang, L. Xu, et al. The Circadian Gene Clock Regulates Bone Formation Via PDIA3. J Bone Miner Res. 2017;32(4):861-871.
25. van den Maagdenberg, A.M., M.H. Hofker, P.J. Krimpenfort, I. de Bruijn, et al. Transgenic mice carrying the apolipoprotein E3-Leiden gene exhibit hyperlipoproteinemia. J Biol Chem. 1993;268(14):10540-5.
26. Schilperoort, M., R. van den Berg, L.A. Bosmans, B.W. van Os, et al. Disruption of circadian rhythm by alternating light-dark cycles aggravates atherosclerosis development in APOE*3-Leiden.CETP mice. J Pineal Res. 2020;68(1):e12614.
27. Yang, X., M. Downes, R.T. Yu, A.L. Bookout, et al. Nuclear receptor expression links the circadian clock to metabolism. Cell. 2006;126(4):801-10.
28. Koorneef, L.L., J.K. van den Heuvel, J. Kroon, M.R. Boon, et al. Selective Glucocorticoid Receptor Modulation Prevents and Reverses Nonalcoholic Fatty Liver Disease in Male Mice. Endocrinology. 2018;159(12):3925-3936.
29. van 't Hof, R.J., L. Rose, E. Bassonga, and A. Daroszewska. Open source software for semi-automated histomorphometry of bone resorption and formation parameters. Bone. 2017;99:69-79.
30. Zimmermann, E.A., C. Riedel, F.N. Schmidt, K.E. Stockhausen, et al. Mechanical competence and bone quality develop during skeletal growth. J Bone Miner Res. 2019;34(8):1461-1472.
31. Aoyama, S. and S. Shibata. The Role of Circadian Rhythms in Muscular and Osseous Physiology and Their Regulation by Nutrition and Exercise. Front Neurosci. 2017;11:63.
32. Tobias, J.H., V. Gould, L. Brunton, K. Deere, et al. Physical Activity and Bone: May the Force be with You. Front Endocrinol (Lausanne). 2014;5:20.
33. Inaoka, T., J.M. Lean, T. Bessho, J.W. Chow, et al. Sequential analysis of gene expression after an osteogenic stimulus: c-fos expression is induced in osteocytes. Biochem Biophys Res Commun. 1995;217(1):264-70.
34. Hirai, T., K. Tanaka, and A. Togari. beta-adrenergic receptor signaling regulates Ptgs2 by driving circadian gene expression in osteoblasts. J Cell Sci. 2014;127(Pt 17):3711-9.
35. Komoto, S., H. Kondo, O. Fukuta, and A. Togari. Comparison of beta-adrenergic and glucocorticoid signaling on clock gene and osteoblast-related gene expressions in human osteoblast. Chronobiol Int. 2012;29(1):66-74.
36. Fujihara, Y., H. Kondo, T. Noguchi, and A. Togari. Glucocorticoids mediate circadian timing in peripheral osteoclasts resulting in the circadian expression rhythm of osteoclast-related genes. Bone. 2014;61:1-9.
37. Brennan, T.A., K.P. Egan, C.M. Lindborg, Q. Chen, et al. Mouse models of telomere dysfunction phenocopy skeletal changes found in human age-related osteoporosis. Dis Model Mech. 2014;7(5):583-92.
38. Willinghamm, M.D., M.D. Brodt, K.L. Lee, A.L. Stephens, et al. Age-related changes in bone structure and strength in female and male BALB/c mice. Calcif Tissue Int. 2010;86(6):470-83.

39. Johannesdottir, F., E. Thrall, J. Muller, T.M. Keaveny, et al. Comparison of non-invasive assessments of strength of the proximal femur. Bone. 2017;105:93-102.
40. Burr, D. and O. Akkus. Bone Morphology and Organization, in Basic and Applied Bone Biology, M.R. Allen, Editor. 2013, Elsevier Inc.: San Diego, United States. p. 3-25.
41. Rouhi, G., W. Herzog, L. Sudak, K. Firoozbakhsh, et al. Free Surface Density Instead of Volume Fraction in the Bone Remodeling Equation: Theoretical Considerations. Forma. 2004;19:165-182.
42. Kivell, T.L. A review of trabecular bone functional adaptation: what have we learned from trabecular analyses in extant hominoids and what can we apply to fossils? J Anat. 2016;228(4):569-94.
43. Follet, H., G. Boivin, C. Rumelhart, and P.J. Meunier. The degree of mineralization is a determinant of bone strength: a study on human calcanei. Bone. 2004;34(5):783-9.
44. Roschger, P., E.P. Paschalis, P. Fratzl, and K. Klaushofer. Bone mineralization density distribution in health and disease. Bone. 2008;42(3):456-66.
45. Neve, A., A. Corrado, and F.P. Cantatore. Osteocalcin: skeletal and extra-skeletal effects. J Cell Physiol. 2013;228(6):1149-53.
46. Tsao, Y.T., Y.J. Huang, H.H. Wu, Y.A. Liu, et al. Osteocalcin Mediates Biomineralization during Osteogenic Maturation in Human Mesenchymal Stromal Cells. Int J Mol Sci. 2017;18(1):159.
47. Busse, B., M. Hahn, M. Soltau, J. Zustin, et al. Increased calcium content and inhomogeneity of mineralization render bone toughness in osteoporosis: mineralization, morphology and biomechanics of human single trabeculae. Bone. 2009;45(6):1034-43.
48. Currey, J.D. Effects of differences in mineralization on the mechanical properties of bone. Philos Trans R Soc Lond B Biol Sci. 1984;304(1121):509-18.
49. Fehrendt, H., T. Linn, S. Hartmann, G. Szalay, et al. Negative influence of a long-term high-fat diet on murine bone architecture. Int J Endocrinol. 2014;2014:318924.
50. Kohsaka, A., A.D. Laposky, K.M. Ramsey, C. Estrada, et al. High-fat diet disrupts behavioral and molecular circadian rhythms in mice. Cell Metab. 2007;6(5):414-21.
51. Alswat, K.A. Gender Disparities in Osteoporosis. J Clin Med Res. 2017;9(5):382-387.
52. Sozen, T., L. Ozisik, and N.C. Basaran. An overview and management of osteoporosis. Eur J Rheumatol. 2017;4(1):46-56.
53. Pouresmaeili, F., B. Kamalidehghan, M. Kamarehei, and Y.M. Goh. A comprehensive overview on osteoporosis and its risk factors. Ther Clin Risk Manag. 2018;14:2029-2049.
54. Alterman, T., S.E. Luckhaupt, J.M. Dahlhamer, B.W. Ward, et al. Prevalence rates of work organization characteristics among workers in the U.S.: data from the 2010 National Health Interview Survey. Am J Ind Med. 2013;56(6):647-59.
55. Parent-Thirion, A., E. Fernández Macías, J. Hurley, and G. Vermeylen. Fourth European Working Conditions Survey. 2007, Luxembourg: Office for Official Publications of the European Communities.

Appendix

Supplementary Table 1. Comparison of the ΔCT amplitude of clock genes and bone-related genes in bones from LD and LD-DL mice.

ΔCT amplitude of genes	LD (mean ± SEM)	LD-DL (mean ± SEM)	P-value
Clock genes			
Rev-erbα	2.01 ± 0.32	-1.97 ± 0.16	**5.63*10-9**
Bmal1	-3.40 ± 0.15	-0.88 ± 0.20	**2.75*10-8**
Clock	-0.76 ± 0.13	-0.30 ± 0.11	**0.013**
Per1	0.49 ± 0.23	0.83 ± 0.33	0.401
Per2	0.93 ± 0.45	1.17 ± 0.31	0.667
Cry1	-0.51 ± 0.21	0.44 ± 0.22	**0.006**
Bone-related genes			
Runx2	-0.47 ± 0.17	-0.01 ± 0.21	0.102
Rankl	-0.80 ± 0.24	-0.71 ± 0.35	0.842
Opg	0.41 ± 0.22	0.01 ± 0.25	0.244
c-Fos	-0.75 ± 0.16	-0.50 ± 0.23	0.381
Nfatc	-0.38 ± 0.15	-0.08 ± 0.22	0.264
Ctsk	-0.53 ± 0.31	-0.09 ± 0.26	0.305

Rhythm amplitude of clock genes and bone-related genes was evaluated by comparing ΔCT (normalized gene expression) amplitude (ZT0 versus ZT12) between LD and LD-DL mice. The P-value of this comparison is shown, and significant P-values ($P < 0.05$) are shown in bold.

Supplementary Table 2. Two-way ANOVA results comparing rhythm in corticosterone and physical activity between LD and LD-DL mice.

	Time effect	Group effect	Interaction
Corticosterone: day 1	**P = 0.0006**	**P = 0.003**	**P < 0.0001**
Corticosterone: day 3	**P < 0.0001**	P = 0.4149	P = 0.2899
Physical activity: day 1	**P = 0.0081**	P > 0.999	**P < 0.0001**
Physical activity: day 3	**P < 0.0001**	P > 0.999	**P < 0.0001**

Significant P-values ($P < 0.05$) are shown in bold.